11.4 Weather Forecasting Applications using WindSat

Thomas Lee, James Goerss, Jeffrey Hawkins, Joseph Turk
Naval Research Laboratory
7 Grace Hopper Avenue
Monterey CA

Zorana Jelenak
NOAA-NESDIS

1. INTRODUCTION

WindSat and QuikSCAT observations were compared against the NRL Atmospheric Variational Data Assimilation System (NAVDAS; Daley and Barker 2001) 10m wind analyses for October 2003-February 2004. The NAVDAS analyses provide the initial conditions for the Navy Operational Global Atmospheric Prediction System (NOGAPS). The WindSat data were derived from an algorithm of Bettenhausen (2006). Only observations of wind speed less than or equal to 20 m/s were considered and only for cases when all flags but the Wind Speed Flag were zero. The QuikSCAT data (Augenbaum et al. 2003) are from the U.S. Navy's Fleet Numerical Meteorology and Oceanography Center (FNMOC) in Monterey California. Only observations for which the wind speed was less than or equal to 20 m/s were considered in cases of zero Rain Flag and zero Edge of Swath Flag. We computed the differences between the observed and analysis wind directions and wind speeds for WindSat and QuikSCAT stratified by NAVDAS analysis wind speed. We computed global statistics for the entire 5-month period and October, December, and February.

The operational NOGAPS/NAVDAS 10m wind analyses for October 2003-February 2004, available at 00, 06, 12, and 18 UTC, provided the baseline for this comparison of WindSat and QuikSCAT vectors. The 10m wind analysis fields come from half-degree global grids at 55 km resolution, the nominal resolution of the NOGAPS T239 spectral forecast model. None of the NOGAPS/NAVDAS analyses include assimilation of satellite ocean surface winds.

* Corresponding author address: Thomas F. Lee, Naval Research Laboratory, Monterey, California 93924, lee@nrlmry.navy.mil

For each analysis time, the WindSat and QuikSCAT observations within a two-hour window centered on the analysis time were compared with the NOGAPS/NAVDAS wind at the satellite retrieval location. Only WindSat and QuikSCAT cases of two or more ambiguities were compared. For both sensors, we selected the observation of wind direction closest to and within 90 degrees of the analysis wind direction at the retrieval location.

For WindSat and QuikSCAT the number of observations totaled about 41 million and 29 million, respectively. 61.3% of the WindSat observations and 60.6% of the QuikSCAT observations occurred when the NOGAPS/NAVDAS wind speed was less than or equal to 7.5 m/s. When the analysis wind speed was less than or equal to 10 m/s, the respective percentages were 83.3% and 81.5%. The results are summarized in Fig. 1. The WindSat standard deviations for speed (top diagram) are smaller than QuikSCAT for wind speeds less than 12.5 m/s or less, a trend reversed above 15 m/s. The wind direction standard deviations for QuikSCAT are comparable to WindSat for wind speeds 7.5 m/s or higher (bottom diagram). For low wind speeds (0 to 7.5 m/s) the Windsat direction standard deviations are artificially lower than QuikScat because of the method used to specify ambiguities. In fact, WindSat direction retrievals have minimal accuracy below about 7 m/s. QuikScat has greater, but still reduced, accuracy at these speeds. Thus, the comparison of the two sensors at the low speeds should not be considered valid.

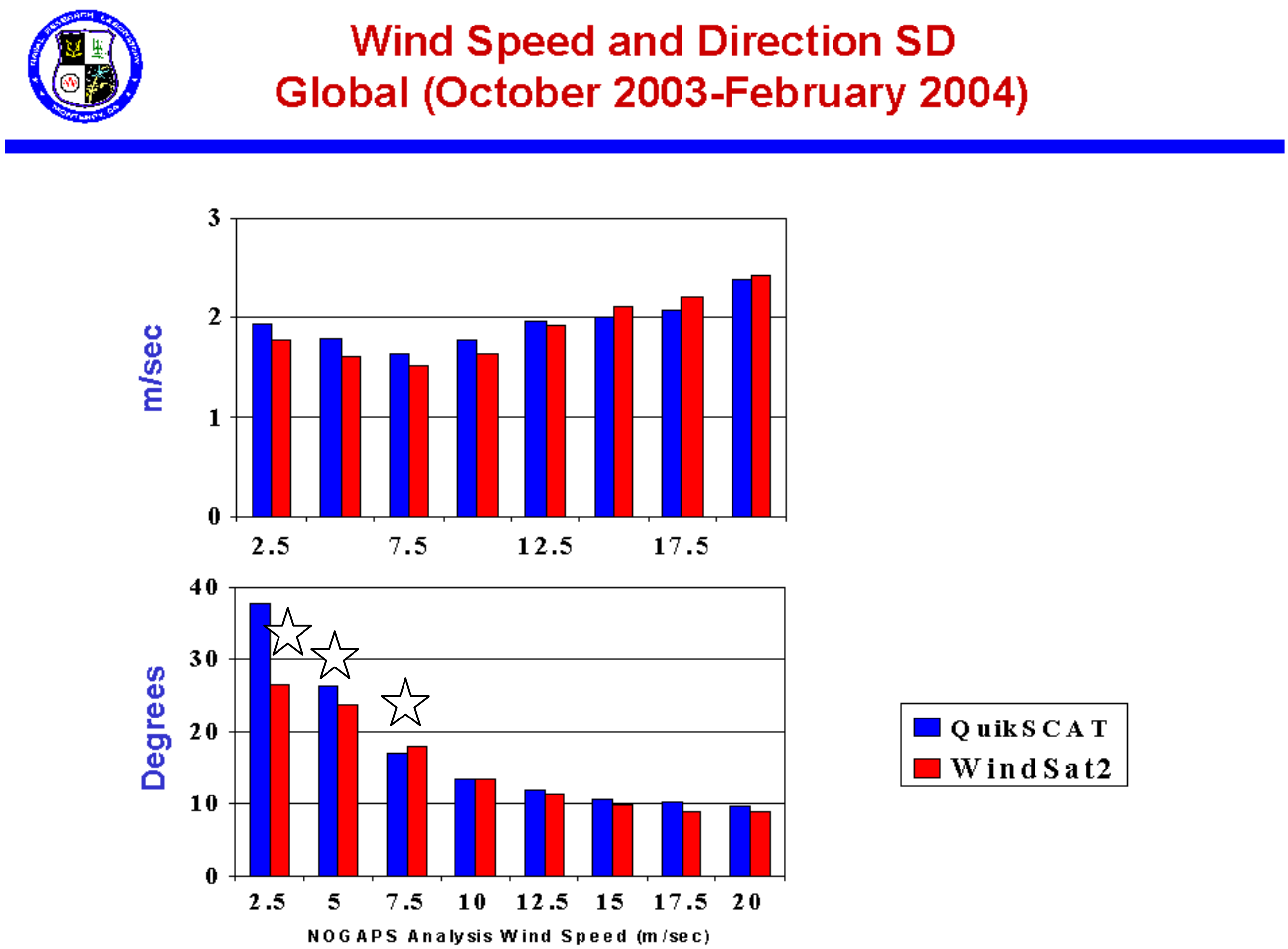

Fig. 1 WindSat and QuikSCAT standard deviations, both with respect to NAVDAS/NOGAPS. Top: Wind speed. Bottom: Wind direction. Stars at low wind speeds (lower diagram) indicates unreliable comparison.

2. CASE STUDIES

A. Rain Contamination in a Frontal System

The version of WindSat retrievals shown in this section is still relatively immature (Version 0; Jelenak et al. 2005), and includes wind vectors, total precipitable water (TPW), total cloud water (TCW), and sea surface temperature. These are shown in Fig. 2A-D. The gradient in TPW identifies the cold front (Katsaros et al. 1989) on the poleward side of a moist plume marking the frontal zone (Fig. 2A). Generally, TCW values higher than 0.2 kg/m2 (darker reds shades on Fig. 2D) indicate probable precipitation and significant wind vector contamination. However, we do not flag contamination on Fig. 2B in order to examine vector behavior in cloudy, rainy regions.

Fortunately, over most of the WindSat pass, the vectors (Fig. 2B) do not occur in regions of high CLW. Within the frontal zone where the retrievals are degraded, wind speeds exceed 50 knots (25 m/s) along the front. These speeds are much higher than nearby retrievals and almost certainly biased high. However, the directions of the 50-knot+ retrievals do not appear entirely unreasonable, marking a shift from northwest west of the front to southwest to the east. Fig. 2C shows sea surface temperature including a sharp gradient (green in the south to blue to the north) showing the boundary of the Gulf Stream. Grey areas mark contamination by significant precipitation, corresponding to regions of high liquid water (and rain) on Fig. 2D.

We have noticed this trend, of high-bias wind speeds but somewhat reasonable directions, in a variety of frontal systems studied with the Version 0 retrievals. This is consistent with the derivation of the wind vectors from the Stokes Vector. The derivation of wind speed comes from the first and second Stokes Vectors. These parameters are very sensitive to atmospheric influence, particularly cloud cover as in Fig. 2D in the frontal zone. Clouds and rain impart a significant high bias to retrieved wind speed values, a similar problem observed in retrievals from the Special Sensor Microwave Imager (SSM/I), a predecessor to WindSat (Goodberlet et al. 1990). However, the retrieval of wind direction is based on the third and fourth Stokes Parameters, which though still sensitive to the atmosphere, are less so than the first and second.

B. Gap Winds as seen in SSM/I and WindSat

Some of the most operationally useful features in WindSat vector plots are due to topographic effects relatively near shore. Although no retrievals are possible closer than about 25-50 km from shore, WindSat represents a major advance in the ability to study coastal winds. Previous passive microwave products showed the wind speeds associated with the gap winds, but wind directions were lacking. For example, a gap wind in an SSM/I image appears in the left side of Fig. 3. It shows a gap wind in the lee of a pass between two major Japanese islands. Directions missing from SSM/I retrievals can be supplied from corresponding model output (Lee and Boyle 1991). However, this is not a satisfactory solution. Despite missing directions, SSM/I winds helped validate mesoscale model forecasts of topographically induced winds (Nachamkin 2004).

When the National Polar Orbiting Environmental Satellite System (NPOESS) Conical Microwave Imager Sounder (CMIS) comes online at the start of the next decade, the ability to observe gap winds will increase substantially. When the NPOESS constellation is fully manifested, three satellites will orbit. CMIS coverage, 1700 km wide, will be substantially greater than Windsat. Due to an extremely fast worldwide data relay system, products will arrive in front of forecasters in 30 min or less after overpass. With retrieval of both speed and direction, CMIS should lead to improvements in mesoscale forecast validation. Data delivery will be even faster at sites capable of direct reception of NPOESS raw data as the satellite passes overhead. Such sites include aircraft carriers of the United States Navy.

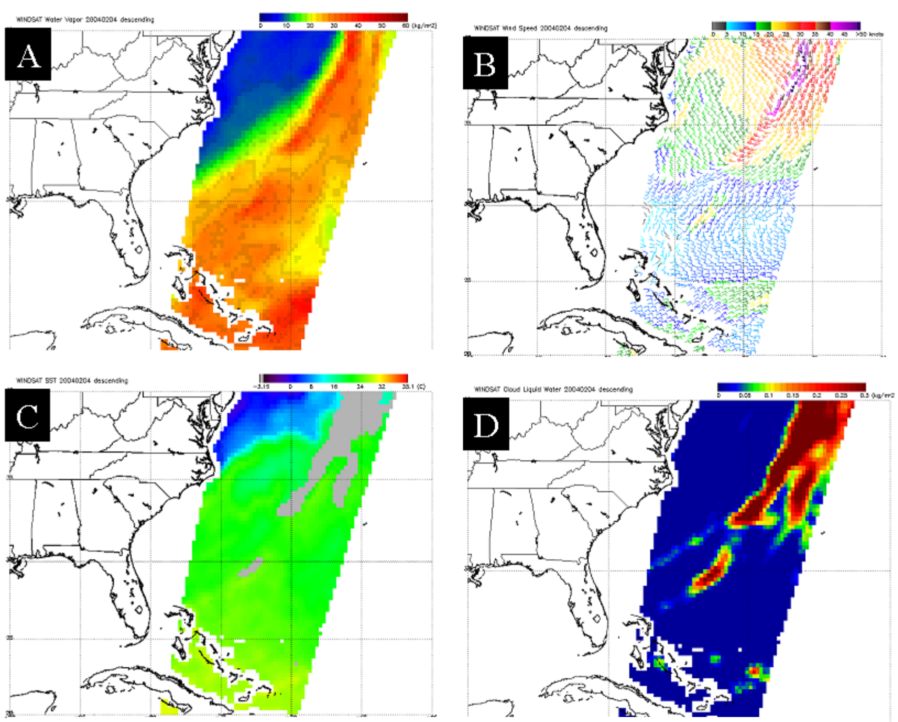

Fig. 2 A) Windsat Total Precipitable Water (kg/m2) 4 February 2004; B) WindSat wind vectors (knots); C) Sea Surface Temperature (C); D. Cloud Liquid Water (kg/m2).

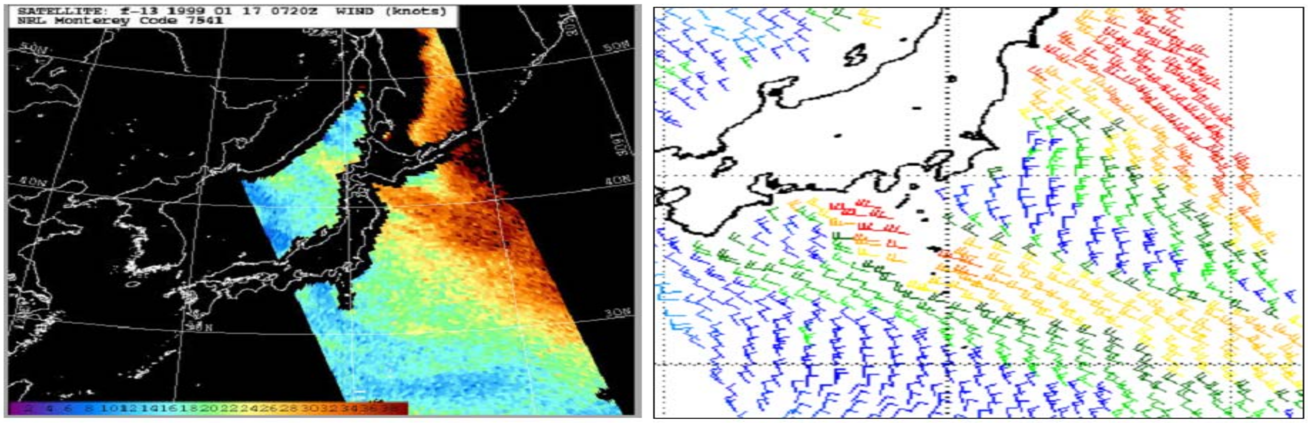

Fig. 3 A) SSM/I wind speed 17 January 1999; B) WindSat wind vectors 18 February 2004. Units in knots.

3. ACKNOWLEDGMENTS

The support of the research sponsor, the National Polar-orbiting Operational Environmental Satellite System's (NPOESS) Integrated Program Office (IPO) located in Silver Spring, MD, is gratefully acknowledged.

4. REFERENCES

Augenbaum, J.M. R.W. Luczak, and G. Legg, 2003: Seawinds near-real-Time processing at NOAA/NESDIS: present status and future plans, *Proceedings American Meteorological Society (Interactive Information and Processing Systems),* Long Beach California, January 2003.

Bettenhausen, M.H., C.K. Smith, R.M. Bevilacqua, N. Wang, P.W. Gaiser, and S. Cox, 2006: A nonlinear optimization algorithm for WindSat wind vector retrievals, *Submitted to IEEE Transactions on Geoscience and Remote Sensing*.

Daley, R. and E. Barker, 2001: NAVDAS: Formulation and Diagnostics, *Mon. Wea. Rev.,* 129, 869-883.

Goodberlet, M.A., C.T. Swift, and J.C. Wilkerson, 1990: Ocean surface wind speed measurements of the Special Sensor Microwave/Imager (SSM/I), *IEEE Trans. Geoscience Remote Sens.,* 28, 823-828.

Jelenak, Z. T. Mavor, L. Connor, N-Y. Wang, P.S. Chang and P. Gaiser, 2005: Validation of ocean wind vector retrievals from WindSat polarimetric measurements, in *Proceedings of 4th International Asian-Pacific Environmental Remote Sensing Conference,* Honolulu HI., 111-121.

Katsaros, K.B., B. Iftekhar, L.A. McMurdie, and G.W. Petty, 1989: Identification of atmospheric fronts over the ocean with microwave measurements of water vapor and rain, *Wea. Forecasting*, 4, 449-460.

Lee, Thomas F., and J.S Boyle, 1991: A synoptic comparison of SSM/I winds with output from an operational forecast system, *Wea. Forecasting*, 6, 404-410.

Nachamkin, J.E., 2004: Mesoscale verification using meteorological composites, *Mon. Wea. Rev.,* 132, 941-955.